

A Thermal Lattice Boltzmann Model for Low Speed Rarefied Gas Flow

Yong-Hao Zhang, Xiao-Jun Gu, Robert W. Barber *and* David R. Emerson

May 2006

© 2006 Council for the Central Laboratory of the Research Councils

Enquiries about copyright, reproduction and requests for additional copies of this report should be addressed to:

Library and Information Services
CCLRC Daresbury Laboratory
Daresbury Warrington
Cheshire WA4 4AD
UK

Tel: +44 (0)1925 603397

Fax: +44 (0)1925 603779

Email: library@dl.ac.uk

ISSN 1362-0207

Neither the Council nor the Laboratory accept any responsibility for loss or damage arising from the use of information contained in any of their reports or in any communication about their tests or investigations.

A Thermal Lattice Boltzmann Model for Low Speed Rarefied Gas Flow

Yong-Hao Zhang, Xiao-Jun Gu, Robert W. Barber, and David R. Emerson

*Center for Microfluidics and Microsystems Modeling,
Department of Computational Science and Engineering,
Council for the Central Laboratory of Research Councils,
Daresbury Laboratory, Warrington, WA4 4AD, UK*

(Dated: May 25, 2006)

Abstract

With development of micro/nano-devices, low speed rarefied gas flows have attracted significant research interest where successful numerical methods for traditional high speed flows including the direct simulation of Monte Carlo method become computationally too expensive. Since the Knudsen number is usually up to the order of unity in a micro/nano flow, one approach is to use continuum methods including the Navier-Stokes-Fourier, Burnett/super Burnett equations, and 13 moments models. Limited success has been achieved because of theoretical difficulties and/or numerical problems. Recently developed lattice Boltzmann equation (LBE) could be another fundamentally different approach close to the kinetic methods but with significantly smaller computational cost. However, despite lattice Boltzmann method is an appealing method for rarefied gas flows at micro/nano scales, there are some hurdles need to be overcome, e.g. capturing velocity slip and temperature jump, predicting stresses and heat flux accurately.

The success of recent attempts of applying LBE model for rarefied gas motion has been mainly focused on isothermal flows. In this paper, thermal rarefied gas flows will be tackled. Because of unique feature of micro/nano flows, a simplified thermal lattice Boltzmann model with two distribution functions can be used. In addition, the kinetic theory boundary condition for the number density distribution function can be extended to construct thermal boundary condition. The model has been validated in the slip flow regime against the solutions of the Navier-Stokes-Fourier equations for shear and pressure driven flows between two planar plates. Moreover, the present thermal LBE model can capture some unique flow characteristics that the Navier-Stokes-Fourier equations fail to predict. The present work indicates that the thermal lattice Boltzmann model is a computationally economic method that is particularly suitable to simulate low speed thermal rarefied gas flows.

PACS numbers: 05.10.-a, 47.45.-n, 47.60.+i

I. INTRODUCTION

In micro/nano-devices, gas flows are characterised rarefied and low speed, i.e. the Knudsen number can be up to the order of unity while the Mach number is negligibly small. Traditionally, research interest for rarefied gas flows has always been for high speed applications where directly solving the Boltzmann equation or the direct simulation Monte Carlo (DSMC) method can offer accurate numerical solutions. However, for low speed gas flows, these methods become computationally too expensive and DSMC suffers large statistical scatter and direction solution of the Boltzmann equation is very complex [1, 2]. Meanwhile, continuum methods such as the Navier-Stokes equations, 13 moment method and the Burnett equations have failed to produce satisfactory results for low-speed gas flows in the transition regime [3]. Despite significant progress has been made in coupling the Navier-Stokes-Fourier (NSF) equations with the BGK model [4], developing the Information Preservation (IP) method for DSMC [5, 6], reducing the statistical scatter associated with Monte Carlo methods [7, 8], no comprehensive and numerically-economical model exists for gas micro/nano-flows with Knudsen numbers up to unity. There is an urgent demand for an efficient and accurate numerical method for low speed rarefied gas flows as often encountered in micro/nano-systems.

Recently, the lattice Boltzmann method has attracted significant interest for simulating micro/nano-flows where the microscopic and macroscopic behaviors are coupled [9–20]. It retains a computational efficiency comparable to Navier-Stokes-Fourier solvers, and is potentially a more accurate model for gas flows over a broad range of Knudsen numbers. While Guo, Zhao and Shi [21] argued that current lattice Boltzmann models cannot be valid in the transition flow regime ($0.1 < Kn < 10$), Sbragaglia et al. [22] have shown that lattice Boltzmann equation (LBE) can be valid for rarefied gas flows with the Knudsen number up to the order of unity. Shan, Yuan and Chen [23] have developed a theoretical framework for higher-order LBE models based on an expansion of the Boltzmann distribution function. However, most work has focused on developing new slip velocity boundary conditions for isothermal flows. Here, we investigate whether a LBE model can produce sufficiently accurate solution for the thermal rarefied gas flows.

II. THERMAL LBE MODEL

Unlike the success of isothermal (athermal) LBE models, thermal LBE models have not been satisfactory in dealing with realistic thermal flows [24]. Because of broad application of thermal flows, continuous effort has been made to construct thermal LBE models and increase numerical stabilities. However, thermodynamically consistent thermal LBE models are still expected, while numerical instability of the current thermal LBE models also defers the model application. Current thermal LBE models may be divided into three categories: multispeed models [25–30], two distribution function models [31–39] and hybrid scheme [40–43]. The multi-speed models use a large set of discrete velocity with higher-order velocity terms in the equilibrium distribution function. Therefore, the macroscopic energy conservation equation can be obtained correctly. These models, however, have suffered numerical instability and the single relaxation time leads to an unphysical fixed Prandtl number. The hybrid schemes employ other methods including a finite difference scheme to solve the temperature equation while the velocity field is determined by the LBE model. This approach does not take advantage of the mesoscopic feature of the LBE methods. The two relaxation time schemes which use two sets of distribution functions for particle number and energy densities to trace velocity and temperature evolution, so that the problems associated with multi-speed models become amenable.

He, Chen and Doolen [35] have established a two-distribution function model which relates the energy density distribution function to the number density distribution function. In addition, viscous heating and compression work are considered in their model. Recently, Shi, Zhao and Guo [38] have proposed an improved model which simplifies the numerical algorithm of He, Chen and Doolen. Whether thermal LBE models are applicable with reasonable accuracy to simulate thermal rarefied gas flows as general and micro/nano flows in particular still remain unknown. Here, a modified two-distribution function model based on refs [35, 38] will be examined to test whether it is suitable to simulate low speed rarefied gas flows. In addition, a kinetic boundary condition for the energy density distribution function will be proposed.

The evolution of both number and energy density distribution functions are given by [35]

$$\frac{\partial f_k}{\partial t} + e_{ki} \frac{\partial f_k}{\partial x_i} = -\frac{f_k - f_k^{eq}}{\lambda} + \frac{(e_{ki} - u_i) F_i}{c_s^2 \rho} f_k^{eq}, \quad (1)$$

and

$$\frac{\partial g_k}{\partial t} + e_{ki} \frac{\partial g_k}{\partial x_i} = -\frac{g_k - g_k^{eq}}{\lambda_t} - f_k q, \quad (2)$$

where f_k and g_k are the distribution functions for the number and energy densities, f_k^{eq} and g_k^{eq} are the distribution functions at equilibrium, e_{ki} is the lattice velocity, u_i is the macroscopic velocity, c_s is the lattice speed of sound, ρ is the density, λ and λ_t are the relaxation times for the number and energy density distribution functions respectively, and q is given by

$$q_k = (e_{ki} - u_i) \cdot \left[\frac{\partial u_i}{\partial t} + e_j \frac{\partial u_i}{\partial x_j} \right]. \quad (3)$$

The relation between two distribution functions is

$$g = \frac{(e_i - u_i)^2}{2} f. \quad (4)$$

The density distribution function at the equilibrium is given by

$$f^{eq} = \rho (2\pi RT)^{-D/2} e^{-(e_i - u_i)^2 / 2RT}, \quad (5)$$

where R is the gas constant and D is the flow dimension. The equilibrium distribution function for the energy density is

$$g^{eq} = \frac{(e_i - u_i)^2}{2} f^{eq}. \quad (6)$$

The macroscopic properties can then be recovered by

$$\begin{aligned} \rho &= \int f de_i, \\ \rho u_i &= \int f e_i de_i, \\ \rho \epsilon &= \int g de_i, \end{aligned} \quad (7)$$

where $\epsilon = DRT/2$.

In discretization of Eqs. (1, 2), He, Chen and Doolen [35] used a second-order temporal scheme to avoid inconsistency of viscosity in the discretized evolution equations for the number and energy density distribution functions. The resulting lattice Boltzmann equations are:

$$\bar{f}_k(\mathbf{x} + \mathbf{e}_k \delta t, t + \delta t) - \bar{f}_k(\mathbf{x}, t) = -\frac{1}{\tau + 0.5} [f_k(\mathbf{x}, t) - f_k^{eq}(\mathbf{x}, t)] + \frac{\tau}{\tau + 0.5} \frac{(e_{ki} - u_i) F_i}{c_s^2 \rho} f_k^{eq}(\mathbf{x}, t), \quad (8)$$

and

$$\bar{g}_k(\mathbf{x} + \mathbf{e}_k \delta t, t + \delta t) - \bar{g}_k(\mathbf{x}, t) = -\frac{1}{\tau_t + 0.5} [\bar{g}_k(\mathbf{x}, t) - g_k^{eq}(\mathbf{x}, t)] - \frac{\tau_t}{\tau_t + 0.5} f_k(\mathbf{x}, t) q_k. \quad (9)$$

where $\tau = \lambda/\delta t$ and $\tau_t = \lambda_t/\delta t$ are the nondimensional relaxation times and δt is the time step. Moreover, two new variables are introduced in order to have an explicit scheme, i.e.

$$\bar{f}_k = f_k + \frac{1}{2\tau} (f_k - f_k^{eq}) - \frac{\delta t (e_{ki} - u_i) F_i}{2 c_s^2 \rho} f_k^{eq}. \quad (10)$$

$$\bar{g}_k = g_k + \frac{1}{2\tau_t} (g_k - g_k^{eq}) + \frac{\delta t}{2} f_k q_k. \quad (11)$$

For a two dimensional nine velocity lattice model (D2Q9), the equilibrium energy distribution functions are

$$\begin{aligned} g_0^{eq} &= -\frac{2\rho\epsilon u_i^2}{9 c_s^2}, \\ g_k^{eq} &= \frac{\rho\epsilon}{9} \left[\frac{3}{2} + \frac{1}{2} \frac{e_{ki} u_i}{c_s^2} + \frac{1}{2} \frac{(e_{ki} u_i)^2}{c_s^4} - \frac{1}{2} \frac{u_i^2}{c_s^2} \right], k = 1 - 4, \\ g_k^{eq} &= \frac{\rho\epsilon}{36} \left[3 + 2 \frac{e_{ki} u_i}{c_s^2} + \frac{1}{2} \frac{(e_{ki} u_i)^2}{c_s^4} - \frac{1}{2} \frac{u_i^2}{c_s^2} \right], k = 5 - 8. \end{aligned} \quad (12)$$

The above complicated scheme is the consequence of eliminating inconsistency of viscosity in the momentum equation and the viscous heating term in the energy equation [35]. In addition, the equilibrium energy distribution function at rest is always negative.

For the gas flows in micro/nano devices considered here, the flow speed is typically very low, i.e. $Ma \ll 1$. Therefore, both compression work and viscous heating are negligibly small. Consequently, the above scheme can be simplified, which has been attempted by Peng, Shu and Chew [44]. However, the equilibrium energy density distribution functions are the same as given by Eq. (12), so that they are negative at rest. Recently, Shi, Zhao and Guo [38] proposed another similar thermal LBE model but with simplified equilibrium distribution function for the energy density. Although the inconsistency of the viscosity in the momentum and energy equations may still remain if viscous heating is not negligible as for high speed gas flows, the simplification approach can be applied for low speed rarefied gas flows. Another advantage of adopting this approach is that the kinetic boundary condition for the energy density distribution at the solid wall can be readily implemented that will be shown later. Following the simplification approach of Shi, Zhao and Guo [38], we can get a thermal LBE model for rarefied gas flows in micro/nano devices, which are given below:

$$f_k(\mathbf{x} + \mathbf{e}_k \delta t, t + \delta t) - f_k(\mathbf{x}, t) = -\frac{1}{\tau} [f_k(\mathbf{x}, t) - f_k^{eq}(\mathbf{x}, t)] + \delta t \frac{(e_{ki} - u_i) F_i}{c_s^2 \rho} f_k^{eq}(\mathbf{x}, t), \quad (13)$$

and

$$g_k(\mathbf{x} + \mathbf{e}_k \delta t, t + \delta t) - g_k(\mathbf{x}, t) = -\frac{1}{\tau_t} [g_k(\mathbf{x}, t) - g_k^{eq}(\mathbf{x}, t)]. \quad (14)$$

If we take D2Q9 model as an example, the lattice velocities are

$$\begin{aligned} e_0 &= 0, \\ e_k &= c(\cos[(k-1)\pi/2], \sin[(k-1)\pi/2]), k = 1-4, \\ e_k &= \sqrt{2}c(\cos[(k-5)\pi/2 + \pi/4], \sin[(k-5)\pi/2 + \pi/4]), k = 5-8, \end{aligned} \quad (15)$$

where $c = \sqrt{3RT}$. And the equilibrium distribution functions for the number density are:

$$\begin{aligned} f_k^{eq} &= \rho \omega_k [1 + \frac{e_{ki} u_i}{c_s^2} + \frac{(e_{ki} u_i)^2}{2c_s^4} - \frac{u_i u_i}{2c_s^2}], \\ \omega_0 &= \frac{4}{9}; \omega_k = \frac{1}{9}, k = 1-4, \omega_k = \frac{1}{36}, k = 5-8. \end{aligned} \quad (16)$$

The equilibrium function for the energy density distribution is:

$$g_k^{eq} = \epsilon f_k^{eq}. \quad (17)$$

In the procedure of deriving above equilibrium energy density distribution functions, the thermal diffusivity α has been modified from $\frac{D+2}{D}(\tau_t - 0.5)c_s^2\delta t$ to $(\tau_t - 0.5)c_s^2\delta t$ [38]. The resulting thermal conductivity k is $\frac{D}{2}R\rho(\tau_t - 0.5)c_s^2\delta t$. The viscosity ν is $(\tau - 0.5)c_s^2\delta t$ so that the second order truncation error is absorbed [35]. Similarly, the second order truncation error is also absorbed by changing thermal diffusivity from $\tau_t c_s^2\delta t$ to $(\tau_t - 0.5)c_s^2\delta t$. The Prandtl number can then be determined as $(\tau - 0.5)/(\tau_t - 0.5)$.

Towards the incompressible limit, the deviatoric stresses are evaluated by the non-equilibrium part of the density distribution function [45]

$$\tau_{ij} = (1 - \frac{1}{2\tau}) \sum_k [f_k(\mathbf{x}, t) - f_k^{eq}(\mathbf{x}, t)] (e_{ki} e_{kj} - \frac{1}{2} e_{ki} e_{ki} \delta_{ij}). \quad (18)$$

The heat flux Q can also be calculated by the non-equilibrium part of the energy distribution function as

$$Q_i = (1 - \frac{1}{2\tau_t}) \sum_k [g_k(\mathbf{x}, t) - g_k^{eq}(\mathbf{x}, t)] e_{ki}. \quad (19)$$

In the rarefied gas flow, we determine the relaxation time from the Knudsen number. For D2Q9 lattice BGK model, the relation between the Knudsen number and the relaxation time is $Kn = \sqrt{\frac{8}{3\pi}} \frac{\tau - 0.5}{N_H}$, where N_H is the number of lattice across the characteristic length

of the flow domain [14]. For a given Prandtl number, we can get the thermal relaxation time. According to the kinetic theory, the mean free path can be related to the viscosity and the mean molecular velocity by

$$\nu = a\bar{c}l, \quad (20)$$

where $a = 0.499$ [46], and $\bar{c} = \sqrt{8RT/\pi}$. The temperature dependent viscosity can be described by:

$$\rho\nu \propto T^\omega, \quad (21)$$

where the value of ω depends on the molecular interaction model, which is between 0.5 for hard sphere interaction and 1 for Maxwellian interaction [46]. Combining Eqs. (20, 21), the influence of temperature variation on the mean free path can be given by

$$\frac{l}{l_{ref}} = \frac{\rho_{ref}}{\rho} \left(\frac{T}{T_{ref}} \right)^{\omega-0.5}, \quad (22)$$

where l_{ref} and ρ_{ref} are the mean free path and density at the reference temperature. Therefore, the local temperature dependent Knudsen number can be determined which couples the lattice Boltzmann equations for the number and energy density distribution functions.

III. BOUNDARY CONDITIONS

In the recent effort on applying LBE models to simulate rarefied gas flows, the focus is on developing slip boundary conditions rather than constructing new LBE models. Currently, there are many types of slip velocity boundary conditions have been used, for examples, bounce-back, specular reflection or a combination of the two [9, 10, 13, 17, 47], kinetic theory boundary conditions [11, 48–50], and a virtual wall collision scheme [18]. For hydrodynamic flows without temperature jump, the bounce back scheme and the nonequilibrium extrapolation method were used as thermal boundary conditions [15, 35, 38]. In this work, we will use the kinetic boundary conditions for diffuse reflection as developed by [11, 48, 51] for slip velocity boundary condition. In addition, we will extend the kinetic boundary condition for the temperature jump at the solid wall.

The kinetic boundary condition for the slip velocity at the wall can be summarised as below:

$$|(\mathbf{e}_k - \mathbf{u}_w) \cdot \mathbf{n}| f_k = \sum_{(\mathbf{e}_{k'} - \mathbf{u}_w) \cdot \mathbf{n} < 0} |(\mathbf{e}_{k'} - \mathbf{u}_w) \cdot \mathbf{n}| R_f(\mathbf{e}_{k'} \rightarrow \mathbf{e}_k) f_{k'}, \quad (23)$$

where k and k' are the reflected and incident directions of the particles, u_w and ρ_w are the velocity and density at the wall, and the scattering kernel is

$$R_f(\mathbf{e}_{k'} \rightarrow \mathbf{e}_k) = \frac{A_N}{\rho_w} [(\mathbf{e}_k - \mathbf{u}_w) \cdot \mathbf{n}] f_k^{eq} |_{\mathbf{u}=\mathbf{u}_w}. \quad (24)$$

A_N is a coefficient given by

$$A_N = \rho_w \frac{\sum_k |(\mathbf{e}_k - \mathbf{u}_w) \cdot \mathbf{n}| f_k}{|(\mathbf{e}_k - \mathbf{u}_w) \cdot \mathbf{n}| f_k^{eq} |_{\mathbf{u}=\mathbf{u}_w} \sum_k |(\mathbf{e}_{k'} - \mathbf{u}_w) \cdot \mathbf{n}| f_{k'}}. \quad (25)$$

In the present thermal LBE model, the equilibrium distribution function for the energy density is given by Eq. (17). The above Maxwellian diffuse reflection at the wall assumes that the reflected particles are in the equilibrium state. Therefore, the reflected energy density distribution function at the wall can be simply related to the reflected number density distribution function by

$$g_k = \frac{DR}{2} T_w f_k. \quad (26)$$

where T_w is the temperature at the solid wall.

IV. RESULTS AND DISCUSSIONS

The present thermal LBE model for gas micro/nano flows is simple in terms of numerical implementation and boundary conditions. In this section, the model will be examined for both shear and pressure driven flows between two infinitely long parallel plates. The

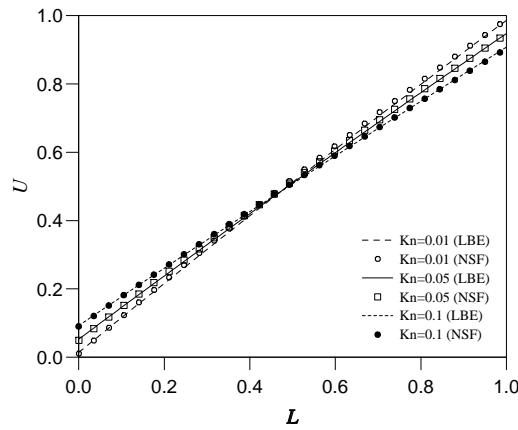


FIG. 1: Nondimensional velocity profiles for planar Couette flow at Knudsen numbers of 0.01, 0.05 and 0.1. Comparison of LBE solution with the NSF slip flow solution.

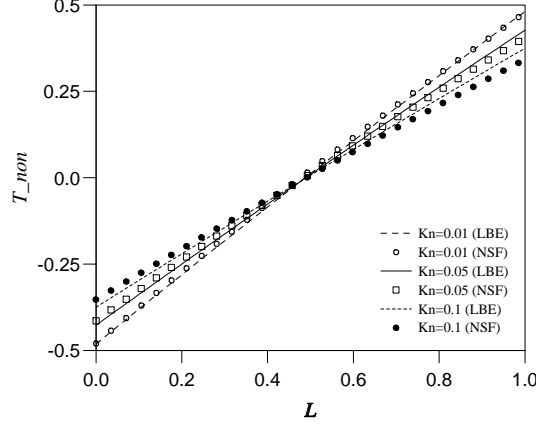


FIG. 2: Nondimensional temperature profiles for planar Couette flow at Knudsen numbers of 0.01, 0.05 and 0.1. Comparison of LBE solution with the NSF slip flow solution.

kinetic boundary conditions given by Eqs. (23, 24, 25, 26) will be used for the gas molecule interactions with the solid wall, while the periodic boundary condition will be used at the inlet and outlet so that only three grid points are needed in the stream direction.

Since experimental data are rare for rarefied gas flows in micro/nano devices, the numerical results of DSMC and directly solving the linearized Boltzmann equation are usually used for model validation. However, for flows with both small Knudsen number and low speed, these methods become not only expensive but also inaccurate. When the Knudsen number is less than 0.1, the Navier-Stokes-Fourier equations with slip boundary conditions can provide results with reasonable accuracy. Therefore, we mainly compare the present thermal LBE solution with the solutions of the Navier-Stokes-Fourier equations in order to test whether the present thermal LBE is valid in the slip flow regime ($0.001 < Kn < 0.1$). The NSF equations for gas flows are summarised below [52]:

$$\frac{\partial \rho}{\partial t} + \nabla \cdot \rho u_i = 0, \quad (27)$$

$$\rho \frac{Du_i}{Dt} = -\frac{\partial p}{\partial x_i} + \frac{\partial}{\partial x_j} \left[2\mu(\phi_{ij} - \frac{1}{3}\phi_{kk}\delta_{ij}) \right], \quad (28)$$

$$\rho \frac{D\epsilon}{Dt} = -p\phi_{ii} + \frac{\partial}{\partial x_i} \left(k \frac{\partial T}{\partial x_i} \right) + 2\mu(\phi_{ij}\phi_{ij} - \frac{1}{3}\phi_{kk}\phi_{ii}), \quad (29)$$

where $\phi_{ij} = \frac{1}{2}(\frac{\partial u_i}{\partial x_j} + \frac{\partial u_j}{\partial x_i})$, δ_{ij} is the Kronecker delta function. Here, both viscosity and thermal conductivity are strongly temperature dependent.

There are velocity slip and temperature jump at the solid surface for nonequilibrium gas flows. The first order slip velocity and temperature jump boundary conditions where the

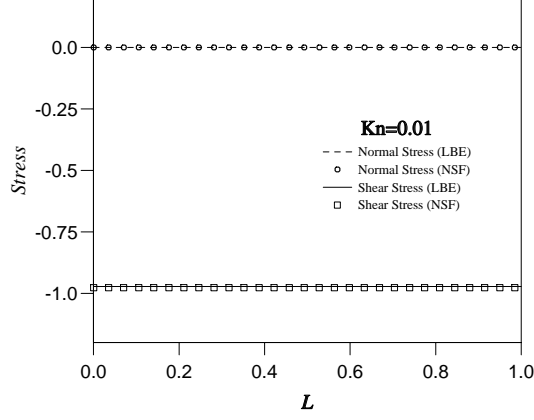


FIG. 3: Nondimensional deviatoric stresses profiles for planar Couette flow at a Knudsen number of 0.01. Comparison of LBE solution with the NSF slip flow solution.

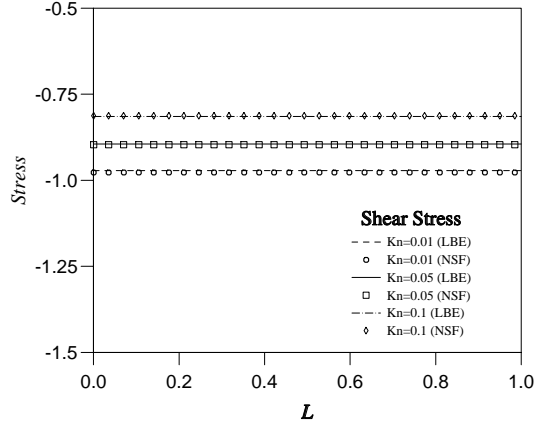


FIG. 4: Nondimensional shear stress profiles for planar Couette flow at Knudsen numbers of 0.01, 0.05 and 0.1. Comparison of LBE solution with the NSF slip flow solution.

gas molecule-wall interactions are assumed diffusely are [53]:

$$u_s - u_w = l \frac{\partial u}{\partial n}, \quad (30)$$

$$T_s - T_w = \frac{2\gamma}{Pr(\gamma + 1)} l \frac{\partial T}{\partial n}, \quad (31)$$

where u_s and T_s are the slip velocity and temperature of the gas at the wall, n is the normal direction of the wall, γ is $\frac{5}{3}$ for a gas without communicable internal energy. Note, the velocity slip and temperature jump coefficients are only weakly correlated with the molecule model[54]. The effect of the molecule model is implemented through the viscosity temperature power law as given by Eq. (21). Through the Prandtl number, the influence of the

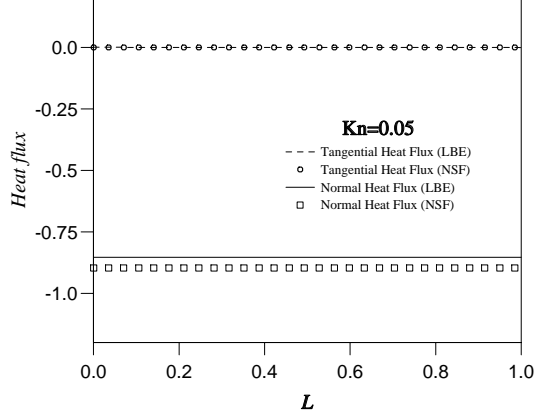


FIG. 5: Nondimensional heat flux profiles for planar Couette flow at a Knudsen number of 0.05. Comparison of LBE solution with the NSF slip flow solution.

temperature on the thermal diffusivity can also be determined. For consistent comparisons, the Maxwellian molecule model will be used for both thermal LBE and Navier-Stokes-Fourier simulations.

In the simulations, the temperature difference at the two plates is ΔT and the mean temperature is T_{ref} . The temperatures at the upper and lower plates are $T_{ref} + \frac{1}{2}\Delta T$ and $T_{ref} - \frac{1}{2}\Delta T$ respectively. L is nondimensional distance defined as $L = x/H$. U is nondimensional velocity, which is defined as $U = u/U_{plate}$ where U_{plate} is the constant moving velocity of the upper plate while the lower plate remains stationary. The velocity of the upper plate is negligibly small in comparison with the sound speed, so that the viscous heating and compression work can be ignored. In the following figures, if not explicitly noted, the temperatures of the lower and upper plates are $0.9T_{ref}$ and $1.1T_{ref}$ respectively.

As shown in Fig. (1), the predictions for the velocity profiles at different Knudsen numbers of the present thermal LBE model and the NSF equations are in excellent agreement. The present thermal LBE can predict not only the slip velocities but also the increasing slip motion with the Knudsen number. In Fig. (2), the profile of the nondimensional temperature T_{non} , which is $(T - T_{ref})/T_{ref}$, is shown. When the Knudsen number is small at 0.01, both thermal LBE model and NSF equations give almost the identical solutions. However, the discrepancy increases with the Knudsen number, especially in the near wall region.

Normal and shear stresses are discussed in Fig. (3), where the Knudsen number is 0.01 and the stresses are nondimensionized by $\mu_{ref}U_{plate}/H$ (μ_{ref} is the viscosity at the reference

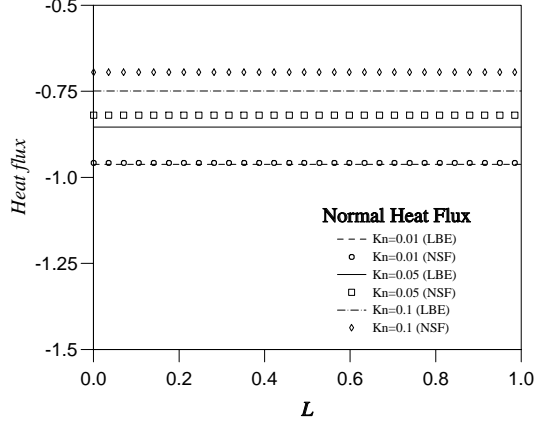


FIG. 6: Nondimensional normal heat flux profiles for planar Couette flow at Knudsen numbers of 0.01, 0.05 and 0.1. Comparison of LBE solution with the NSF slip flow solution.

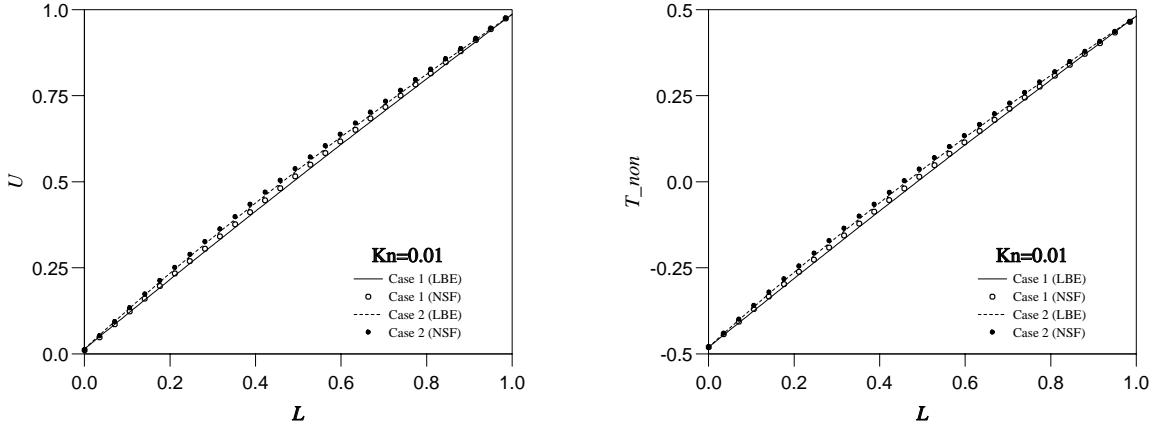


FIG. 7: The effect of temperature variation on the nondimensional velocity and temperature profiles for planar Couette flow at a Knudsen number of 0.01. Comparison of LBE solution with the NSF slip flow solution.

temperature). Both thermal LBE model and NSF equations predict a zero normal stress, which is also true for flows with other Knudsen numbers. If there is no slip motion at the wall, the nondimensional shear stress will be unity. Because of slip motion, the magnitude of the shear stress is now less than 1.0 despite it is still constant across the two plates. As shown in Fig. (4), the magnitude of the shear stresses decreases with increasing Knudsen number which is due to increasing slip velocity. Again, excellent agreements have been observed for the stresses profiles predicted by the thermal LBE and the NSF equations.

In Fig. (5) and Fig. (6), the temperature is nondimensionized by $k_{ref}\Delta T/H$, where k_{ref}

is the thermal conductivity at the reference temperature. Fig. (5) shows that the tangential heat flux, which is the heat flux in the flow direction, is zero because the viscous heating and compression work are negligible. Therefore, only heat flux in the normal direction is compared in Fig. (6). When Kn is 0.01, the solution of the thermal LBE model agrees well with the prediction of the NSF equations. However, the discrepancy grows with increasing Knudsen number. Again, because of temperature jump at the wall, the magnitude of heat flux in the normal direction is smaller than otherwise unity. In addition, both thermal LBE model and NSF equations can predict a decreasing magnitude of the normal heat flux with increasing Knudsen number, i.e. increasing temperature jumps.

Because both viscosity and thermal conductivity depend strongly on the temperature, we have examined the effect of the temperature on the velocity and temperature profiles in Fig. (7). The temperatures at the upper and lower plates are $0.9T_{ref}$ and $1.1T_{ref}$ in the Case 1, and $0.7T_{ref}$ and $1.3T_{ref}$ in the Case 2. It is clearly demonstrated that the large temperature drop between the two plates will cause the maximum velocity to be shifted towards the cold plate and a larger deviation of the temperature profile from the linear one. This test case shows that the present thermal LBE model is capable of simulating thermal flows with large temperature variation.

Overall, the present thermal LBE performs well in the slip flow regime for the Couette flows. Since the NSF equations become inappropriate when the Knudsen number is beyond 0.1, the deviation from the solutions of the NSF equations at large Knudsen number needs further investigation.

V. CONCLUSIONS

The present thermal LBE model has advantages of simple algorithm and numerical efficiency for low speed rarefied gas flows. The model results are in excellent agreement with the solutions of the NSF equations in the slip flow regime. Moreover, the present model can capture high-order rarefaction effect in the heat flux which the NSF equations fail. Therefore, it offers an ideal numerical simulation tool for low speed rarefied gas system simulation as encountered in micro/nano devices. In the next step, we will investigate whether a thermal LBE model based on the present work can be applied to simulate low speed rarefied gas flow in the transition regime with the Knudsen number up to the order of unity.

VI. ACKNOWLEDGEMENTS

This work is financially supported by UK Engineering and Physical Sciences Research Council (EPSRC) under grant reference no. GR/S82978/01. Additional support was provided by EPSRC under the auspices of Collaborative Computational Project 12 (CCP12).

- [1] N. G. Hadjiconstantinou, A. Garcia, M. Bazant, and G. He, *J. Comput. Phys.* **187**, 274 (2003).
- [2] F. Sharipov, L. M. G. Cumin, and D. Kalempa, *Euro. J. Mech. B-Fluid* **23**, 899 (2004).
- [3] C. L. Bailey, R. W. Barber, and D. R. Emerson, in *European Congress on Computational Methods in Applied Sciences and Engineering, ECCOMAS 2004*, edited by P. Neittaanmäki, T. Rossi, S. Korotov, E. Oñate, J. Périaux, and D. Knörzer (Jyväskylä, Finland, 2004).
- [4] K. Xu and Z. Li, *J. Fluid Mech.* **513**, 87 (2004).
- [5] J. Fan and C. Shen, *J. Comp. Phys.* **167**, 393 (2001).
- [6] Q. Sun and I. D. Boyd, pp. AIAA-2005-4828 (2005).
- [7] L. L. Baker and N. G. Hadjiconstantinou, *Phys. Fluids* **17**, 051703 (2005).
- [8] J. Chun and D. L. Koch, *Phys. Fluids* **17**, 107107 (2005).
- [9] X. B. Nie, G. Doolen, and S. Chen, *J. Stat. Phys.* **107**, 279 (2002).
- [10] C. Y. Lim, C. Shu, X. D. Niu, and Y. T. Chew, *Phys. Fluids* **14**, 2299 (2002).
- [11] X. D. Niu, C. Shu, and Y. T. Chew, *Europhys. Lett.* **67**, 600 (2004).
- [12] T. Lee and C.-L. Lin, *Phys. Rev. E* **71**, 046706 (2005).
- [13] Y. H. Zhang, R. S. Qin, and D. R. Emerson, *Phys. Rev. E* **71**, 047702 (2005).
- [14] Y. H. Zhang, R. S. Qin, Y. H. Sun, R. W. Barber, and D. R. Emerson, *J. Stat. Phys.* **121**, 257 (2005).
- [15] G. H. Tang, W. Q. Tao, and Y. L. He, *Phys. Rev. E* **72**, 056301 (2005).
- [16] G. H. Tang, W. Q. Tao, and Y. L. He, *Phys. Rev. E* **72**, 016703 (2005).
- [17] M. Sbragalia and S. Succi, *Phys. Fluids* **17**, 093602 (2005).
- [18] F. Toschi and S. Succi, *Europhys. Lett.* **69**, 549 (2005).
- [19] V. Sofonea and R. F. Sekerka, *J. Comp. Phys.* **207**, 639 (2005).
- [20] V. Sofonea and R. F. Sekerka, *Phys. Rev. E* **71**, 066709 (2005).

- [21] Z. L. Guo, T. S. Zhao, and Y. Shi, J. Appl. Phys. **99**, 074903 (2006).
- [22] M. Sbragalia and S. Succi, Europhys. Lett. **73**, 370 (2006).
- [23] X. Shan, X.-F. Yuan, and H. Chen, J. Fluid Mech. **550**, 413 (2006).
- [24] P. Lallemand and L.-S. Luo, Phys. Rev. E **68**, 036706 (2003).
- [25] F. J. Alexander, S. Chen, and J. D. Sterling, Phys. Rev. E **47**, R2249 (1993).
- [26] Y. Chen, H. Ohashi, and M. Akiyama, Phys. Rev. E **50**, 2776 (1994).
- [27] G. McNamara, A. Garcia, and B. Alder, J. Stat. Phys. **81**, 395 (1995).
- [28] P. Pavlo, G. Vahala, and L. Vahala, Phys. Rev. Lett. **80**, 3960 (1998).
- [29] P. Pavlo, G. Vahala, L. Vahala, and M. Soe, J. Comput. Phys. **139**, 79 (1998).
- [30] P. Pavlo, G. Vahala, and L. Vahala, J. Stat. Phys. **107**, 499 (2002).
- [31] A. Bartoloni, C. Battista, S. Cabasino, P. S. Paolucci, J. Pech, R. Sarno, G. M. Todesco, M. Torelli, W. Tross, P. Vicini, et al., Int. J. Mod. Phys. C **4**, 993 (1993).
- [32] J. G. M. Eggels and J. A. Somers, J. Heat Fluid Flow **16**, 357 (1995).
- [33] X. Shan, Phys. Rev. E **55**, 2780 (1997).
- [34] R. G. M. van der Sman, Int. J. Mod. Phys. C **8**, 879 (1997).
- [35] X. He, S. Chen, and G. Doolen, J. Comp. Phys. **146**, 282 (1998).
- [36] B. J. Palmer and D. R. Rector, J. Comp. Phys. **161**, 1 (2000).
- [37] Z. L. Guo, B. C. Shi, and C. G. Zheng, Int. J. Numer. Methods Fluids **39**, 325 (2002).
- [38] Y. Shi, T. S. Zhao, and Z. L. Guo, Phys. Rev. E **70**, 066310 (2004).
- [39] Y. Shi, T. S. Zhao, and Z. L. Guo, Comp. Fluids **35**, 1 (2006).
- [40] O. Filippova and D. Hänel, Int. J. Mod. Phys. C **9**, 1439 (1998).
- [41] O. Filippova and D. Hänel, J. Comput. Phys. **158**, 139 (2000).
- [42] P. Lallemand and L.-S. Luo, Int. J. Mod. Phys. B **17**, 41 (2003).
- [43] A. Al-Zoubi and G. Brenner, Int. J. Mod. Phys. C **15**, 307 (2004).
- [44] Y. Peng, C. Shu, and Y. T. Chew, Phys. Rev. E **68**, 026701 (2003).
- [45] D. Yu, R. Mei, L.-S. Luo, and W. Shyy, Prog. Aerospace Sci. **39**, 329 (2003).
- [46] S. Chapman and T. G. Cowling, *The mathematical theory of non-uniform gases* (Cambridge University Press, Cambridge, 1975).
- [47] S. Succi, Phys. Rev. Lett. **89**, 064502 (2002).
- [48] S. Ansumali and I. V. Karlin, Phys. Rev. E **66**, 026311 (2002).
- [49] G. H. Tang, W. Q. Tao, and Y. L. He, Phys. Fluids **17**, 058101 (2005).

- [50] X. D. Niu, C. Shu, and Y. T. Chew, J. Comp. Phys. (2006).
- [51] R. Gatignol, Phys. Fluids **20**, 2022 (1977).
- [52] G. K. Batchelor, *An introduction to fluid dynamics* (Cambridge University Press, Cambridge, 1967).
- [53] M. Gad-el-Hak, J. Fluids Eng. **121**, 5 (1999).
- [54] C. Cercignani, *The Boltzmann equation and its applications* (Springer-Verlag, New York, 1988).



Council for the Central Laboratory of the Research Councils

Chilton, Didcot, Oxfordshire OX11 0QX, UK

Tel: +44 (0)1235 445000 Fax: +44 (0)1235 445808

**CCLRC Rutherford Appleton
Laboratory**

Chilton, Didcot,
Oxfordshire OX11 0QX
UK

Tel: +44 (0)1235 445000

Fax: +44 (0)1235 44580

CCLRC Daresbury Laboratory

Keckwick Lane
Daresbury, Warrington
Cheshire WA4 4AD
UK

Tel: +44 (0)1925 603000

Fax: +44 (0)1925 603100

CCLRC Chilbolton Observatory

Drove Road
Chilbolton, Stockbridge
Hampshire SO20 6BJ
UK

Tel: +44 (0)1264 860391

Fax: +44 (0)1264 860142



INVESTOR IN PEOPLE